

N-Carbamidoyl-4-((3-ethyl-2,4,4-trimethylcyclohexyl)methyl)benzamide Enhances Staurosporine Cytotoxic Effects Likely Inhibiting the Protective Action of Magmas toward Cell Apoptosis

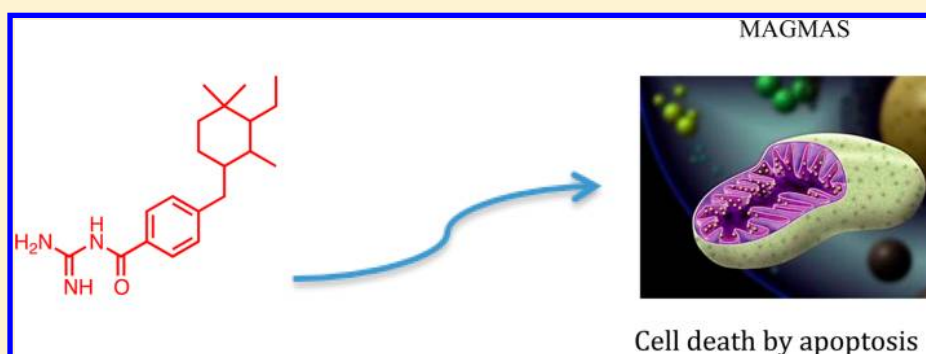
Maria Chiara Zatelli,^{†,‡,||} Teresa Gagliano,^{†,||} Michela Pelà,[§] Sara Bianco,[§] Valerio Bertolasi,[§] Federico Tagliati,[†] Remo Guerrini,^{‡,§} Ettore degli Uberti,^{†,‡} Severo Salvadori,^{‡,§} and Claudio Trapella^{*,‡,§}

[†]Section of Endocrinology, Department of Medical Sciences, University of Ferrara, 44121 Ferrara, Italy

[‡]Laboratorio in Rete del Tecnopolo Tecnologie delle Terapie Avanzate (LTTA), University of Ferrara, 44121 Ferrara, Italy

[§]Department of Chemical and Pharmaceutical Sciences, University of Ferrara, Via Fossato di Mortara 17, 44121 Ferrara, Italy

Supporting Information



ABSTRACT: We recently demonstrated that Magmas overexpression protects GH-secreting rat pituitary adenoma cell lines from apoptosis by inhibiting cytochrome *c* release from mitochondria after treatment with staurosporine, strongly suggesting a role of Magmas in preventing apoptosis. The aim of this study was to produce a drug that, by inhibiting Tim16, may sensitize chemoresistant tumor cell to proapoptotic stimuli. We synthesized six compounds and challenged their sensitizing effects toward the proapoptotic effects of staurosporine in the TT cell line, derived from a human medullary thyroid carcinoma. We found that compound **5**, devoid of the planarity in the aliphatic part of the lead **1**, is not cytotoxic but enhances the proapoptotic effects of staurosporine by reducing MMP activation. Compound **5** may be useful for cancer treatment in association with chemotherapeutic drugs, possibly allowing a reduction of the chemotherapeutic agent effective dose.

■ INTRODUCTION

Magmas (mitochondria-associated protein involved in granulocyte-macrophage colony-stimulating factor signal transduction) gene encodes for the mitochondrial protein Tim 16, a member of the translocase complex TIM23, located in the mitochondrial inner membrane. Tim 16 drives proteins from the intermembrane space into the mitochondrial matrix by functionally interacting with Tim 14, a protein participating in the TIM23 complex.¹

Magmas was found to be overexpressed in prostate cancer, suggesting a role for this gene in tumor development.² In keeping with these findings, we previously demonstrated that Magmas is overexpressed in human pituitary adenomas as well as in ACTH-secreting mouse pituitary adenoma cell lines compared to their respective human and murine normal counterparts. We found that Magmas silencing sensitizes ACTH-secreting mouse pituitary adenoma cell lines to proapoptotic stimuli and induces an accumulation in the G0/

G1 phase of the cell cycle,³ supporting the hypothesis that Magmas may play a role in tumor development by protecting neoplastic cells from apoptosis and by promoting cell proliferation. The protective role of Magmas toward apoptotic stimuli was also confirmed in GH-secreting rat pituitary adenoma cell lines, where Magmas overexpression protects from apoptosis by inhibiting staurosporine-induced cytochrome *c* release from mitochondria.⁴ These data point to a role for Magmas in tumor resistance to proapoptotic stimuli (such as chemotherapeutic drugs), indicating that Magmas inhibition may represent a successful strategy to overcome chemoresistance. A consolidated in vitro model of chemoresistance is represented by the TT cell line, derived from a human medullary thyroid carcinoma (MTC), that displays resistance to chemotherapeutic drugs and to apoptotic stimuli.^{5–7} TT cells display an

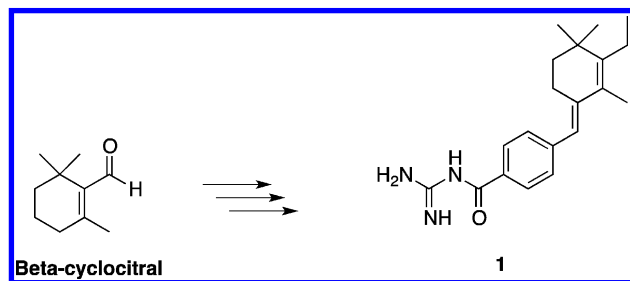
Received: January 10, 2014

Published: April 24, 2014

activating RET mutation⁸ that leads to constitutive p38MAPK signaling that, in turn, confers resistance to apoptosis.⁹ MTC is an aggressive tumor arising from thyroid parafollicular C cells that, to date, is orphan of an effective medical therapy, since classic chemotherapy or radiation therapy is seldom effective in controlling disease progression.¹⁰

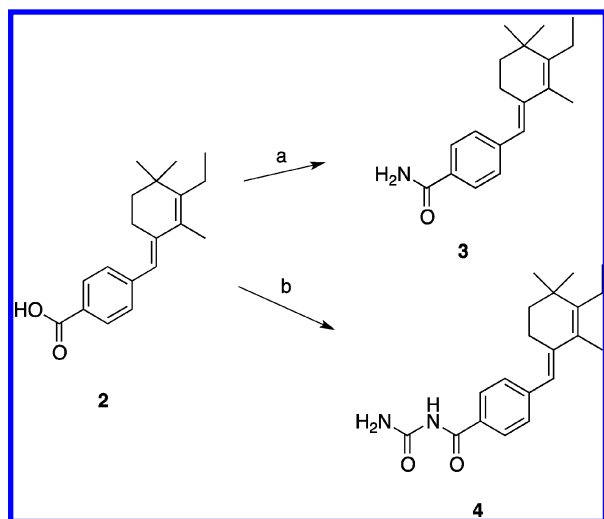
We therefore aimed at synthesizing a chemical inhibitor of Tim 16, starting from a previously synthesized compound (referred to as compound 1)¹¹ (Scheme 1), evaluating its capability of sensitizing a chemoresistant cell line, the TT cells, to proapoptotic stimuli.

Scheme 1



RESULTS

Synthesis. The synthesis of compound 1, which was demonstrated to reduce yeast proliferation *in vitro*, was achieved as previously reported.¹¹ On the basis of these data, we decided to perform a SAR study of the molecule, investigating in particular the polar function (guanidine) and the planarity of its aliphatic portion. As depicted in Scheme 2,

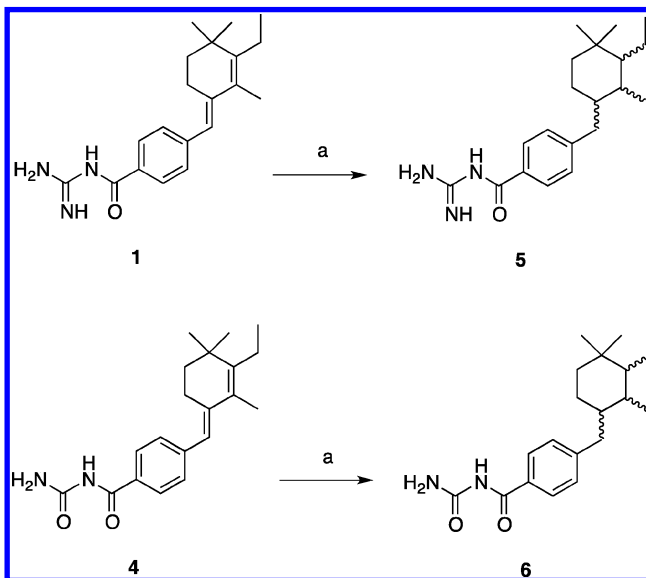
Scheme 2^a

^aConditions: (a) DMF, CDI, NH₄OH, 24 h, Y = 20%; (b) toluene, urea, 3,4,5 trifluoromethylphenylboronic acid, reflux, 24 h, Y = 45%.

we started from acid derivative 2 to prepare the corresponding primary amide 3 and urea 4. The amide preparation was achieved by carbonyldiimidazole activation of the corresponding carboxylate and subsequent reaction with concentrated ammonia solution to yield amide 3 after crystallization from diethyl ether. The urea derivative 4 was obtained from acid 2 by

reaction with urea in the presence of trifluoromethylboronic acid as a catalyst.¹²

To better understand the role of planarity in the aliphatic portion of the molecule, we decided to reduce both endocyclic and exocyclic double bonds by catalytic hydrogenation as depicted in Scheme 3, obtaining compound 5. The same reduction was done for the corresponding urea 4 to obtain compound 6.

Scheme 3^a

^aConditions: (a) EtOH/EtOAc 1:1, C/Pd, H₂, 1 atm, 12 h, 97% for 5, 82% for 6.

Magmas Expression in TT Cell Line. The TT cell line was characterized for Magmas expression. As shown in Figure 1A, Tim 16, the protein encoded by the Magmas gene, is expressed in TT cells, with the expected molecular weight (13,8 kDa), to a greater extent compared to normal thyroid tissue (NT).

As shown in Figure 1B, Tim 16 protein levels were not influenced in TT cells by treatment with each compound alone or in combination with staurosporine.

Effects of Compounds on Cell Viability and Apoptosis. We evaluated the ability of the synthesized compounds (compounds 1, 2, 3, 4, 5, and 6) to influence TT cell viability. As shown in Figure 2A, compound 1 significantly ($P < 0.01$) reduced cell viability at 10 μ M concentration. On the contrary, compounds 2, 3, 4, and 5 did not influence this parameter. In order to verify whether the reduction in cell viability was due to the induction of apoptosis, caspase 3/7 activation was evaluated. As shown in Figure 2B, 10 μ M compound 1 significantly ($P < 0.01$) induced caspase activation, while compounds 2, 3, 4, and 5 did not significantly modify this parameter in TT cells. These results indicate that compound 1 at higher concentration reduces cell viability and promotes apoptosis in TT cells. On the contrary, all the other compounds did not affect these parameters in basal conditions.

Effects of Compounds in Promoting Apoptotic Stimuli Action. To investigate the possible role of Magmas inhibitors in enhancing apoptosis activation under apoptotic stimuli, TT cells were treated with compounds 1, 2, 3, 4, and 5 at 5 or 10 μ M with or without 50 nM staurosporine.

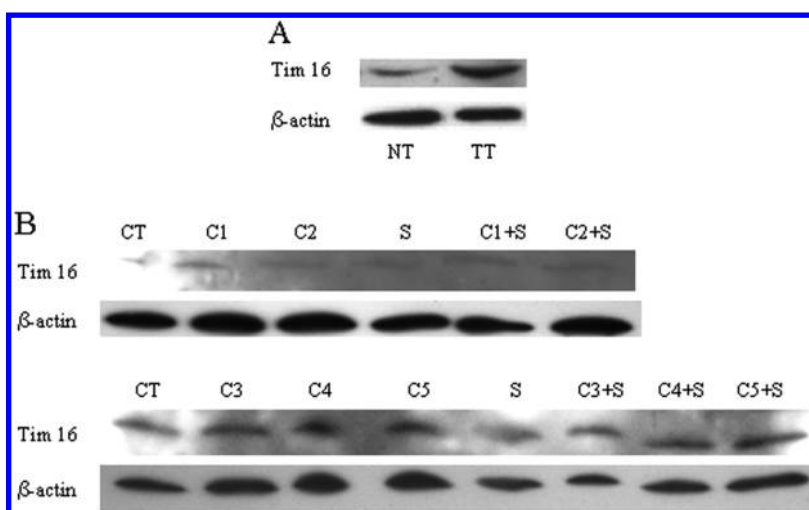


Figure 1. (A) Total proteins were isolated from TT cells and from a pool of normal thyroid tissues (NT), and Western blot analysis for Tim 16 protein expression was performed. β -Actin is shown as loading control. (B) TT cells were treated with compounds 1–5 (C1, C2, C3, C4, C5) at 10 μ M alone or in combination with 50 nM staurosporine (S) for 24 h and then harvested. Total proteins were isolated, and Western blot analysis for Tim 16 protein expression was performed. β -Actin is shown as loading control.

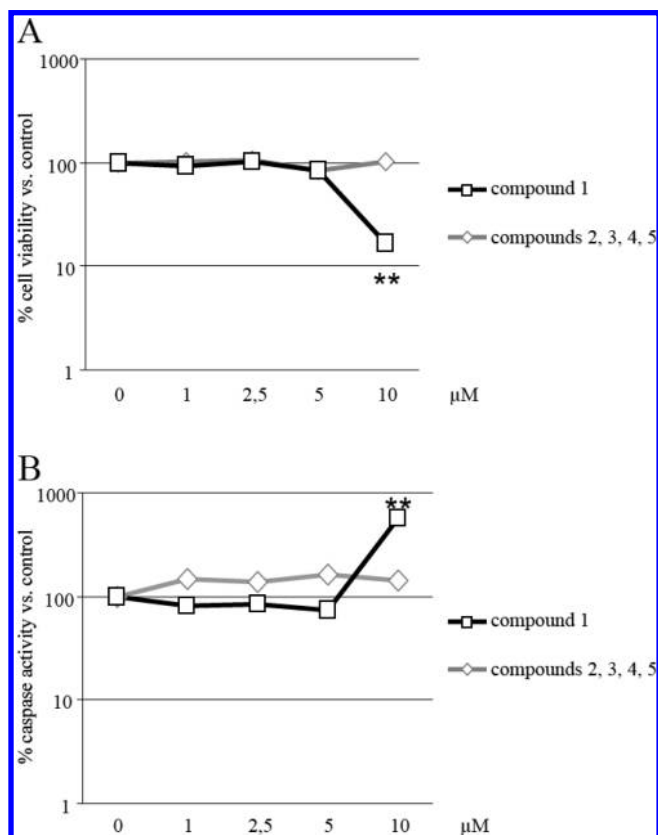


Figure 2. Effects of compounds 1, 2, 3, 4, and 5 on cell viability and apoptosis. TT cells were treated with increasing doses (1–10 μ M) of compound 1 (black line) or compound 2, 3, 4, or 5 (gray line), renewing the treatment every 24 h. After 72 h, cell viability was measured by ATPlite assay (A) and apoptosis activation was measured by caspase 3/7 assay (B). ** indicates $P < 0.01$ vs control cells.

As shown in Figure 3A (left panel), staurosporine significantly reduced TT cell viability (by 63%; $P < 0.01$). In keeping with previous results, compound 1 at 10 μ M, but not at 5 μ M, significantly reduced cell viability (by $\sim 70\%$; $P < 0.01$ vs control). In addition, 5 and 10 μ M compound 1 significantly (P

< 0.01) enhanced the inhibitory effects of staurosporine on cell viability. To verify whether the reduction in cell viability was associated with apoptotic mechanisms, apoptosis activation was evaluated by measuring caspase 3/7 activity in the same conditions. As shown in Figure 3A (right panel), staurosporine significantly ($P < 0.01$) induced caspase 3/7 activation (200% vs control cells). In line with the results on cell viability, compound 1 at 10 μ M, but not at 5 μ M, significantly induced caspase 3/7 activation (by $\sim 300\%$; $P < 0.01$ vs control). In addition, 5 and 10 μ M compound 1 significantly ($P < 0.01$) enhanced the stimulatory effects of staurosporine on caspase activation by 40% and 400%, respectively.

As shown in Figure 3B (left panel), 5 and 10 μ M compound 2 did not significantly modify cell viability nor significantly enhanced staurosporine antiproliferative effects. Accordingly, 5 and 10 μ M compound 2 did not significantly modify caspase 3/7 activity nor significantly enhanced staurosporine-induced apoptosis activation (Figure 3B, right panel). Similar results were obtained when TT cells were challenged with compound 3 (Figure 3C) and compound 4 (Figure 3D), concerning both cell viability (left panels) and caspase activation (right panels). In keeping with previous results, compound 5 alone did not affect cell viability but was capable of enhancing the inhibitory effects of staurosporine on cell viability at both concentrations tested (by 12% and 20%, respectively; $P < 0.05$) (Figure 3E, left panel). Similarly, compound 5 alone did not affect caspase 3/7 activation but was capable of potentially enhancing the stimulatory effects of staurosporine on this parameter (+140% and +330% with 5 and 10 μ M, respectively; $P < 0.01$) (Figure 3E, right panel).

These data indicate that both compound 1 and compound 5 are capable of sensitizing TT cells to the proapoptotic effects of staurosporine. However, while compound 1 displays a cytotoxic action, the latter is not exerted by compound 5, which, per se, does not significantly alter basal TT cell viability and caspase 3/7 activation.

As shown in Figure 4A, staurosporine significantly reduced MCF12A cell viability (by 53%; $P < 0.01$). In keeping with previous results, compound 5 at 5 and 10 μ M did not significantly affect cell viability and did not enhance the

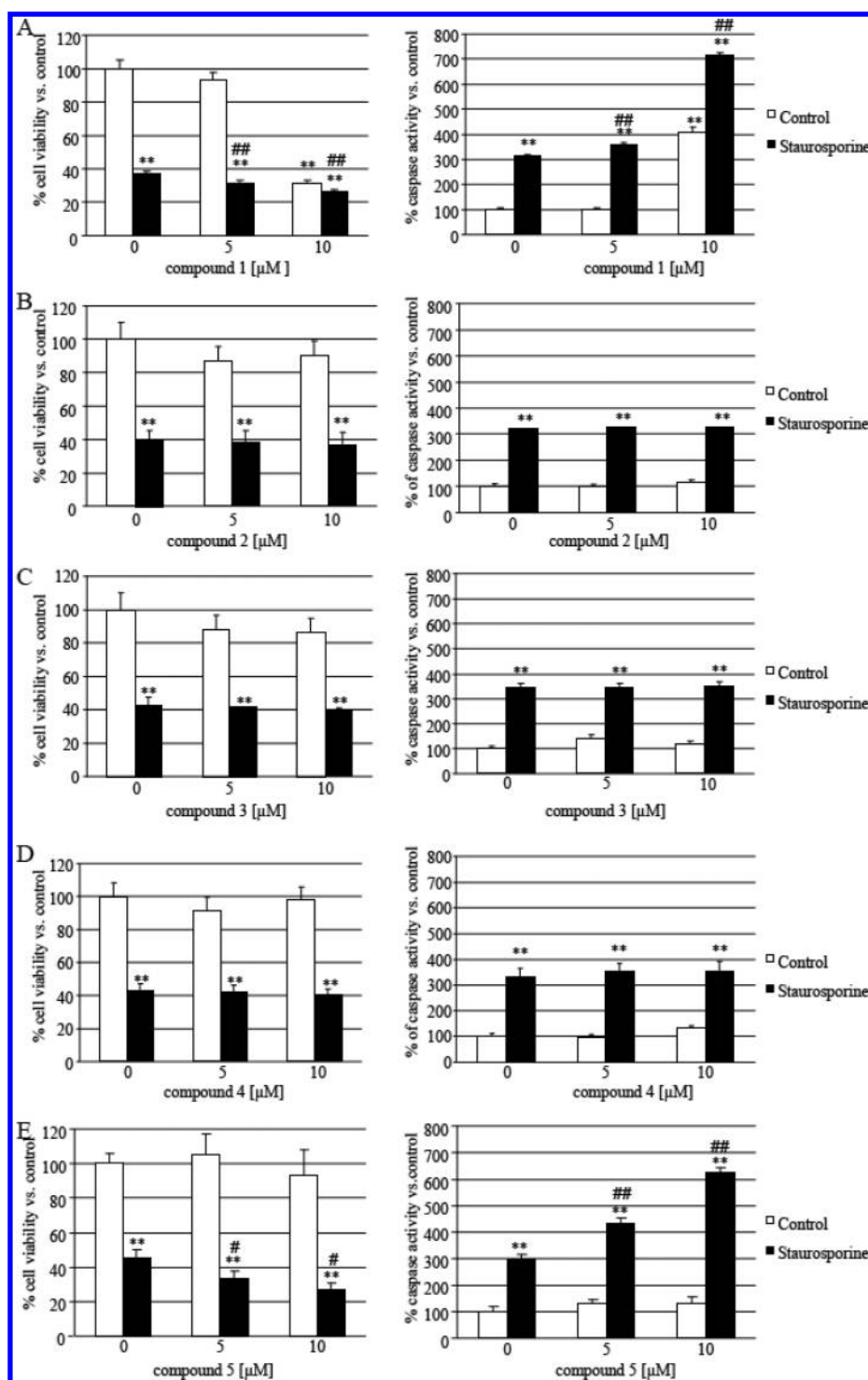


Figure 3. Effects of compounds 1, 2, 3, 4, and 5 at 5 and 10 μM in combination with staurosporine 50 nM on cell viability and apoptosis. Left panels: TT cells were treated without or with 5 or 10 μM indicated compounds (white bars) alone or in combination with 50 nM staurosporine (black bars). Treatments were renewed every 24 h, and cell viability was evaluated after 72 h. Right panels: TT cells were treated with 5 or 10 μM indicated compounds (white bars) alone or in combination with 50 nM staurosporine (black bar). Treatments were renewed every 24 h, and caspase 3/7 activity was evaluated after 72 h. ** indicates $P < 0.01$ vs control cells. # indicates $P < 0.05$ and ## indicates $P < 0.01$ vs staurosporine-treated cells.

antiproliferative effects of staurosporine. In addition, Tim16 protein levels are much lower in MCF12A cells compared to TT cells (Figure 4B).

Effects of Compounds 1 and 5 on Mitochondrial Membrane Potential. We then evaluated the ability of Magmas inhibitors to influence mitochondrial membrane potential (MMP). Since compounds 2, 3, and 4 did not

display any sensitizing effect toward the proapoptotic action of staurosporine, MMP was tested in TT cells only under treatment with compound 1 and compound 5. TT cells were treated with 50 nM staurosporine alone or in combination with either 10 μM compound 1 or 10 μM compound 5 and then submitted to MMP evaluation by using Jc-1 assay. As shown in Figure 5, staurosporine alone dramatically reduced red

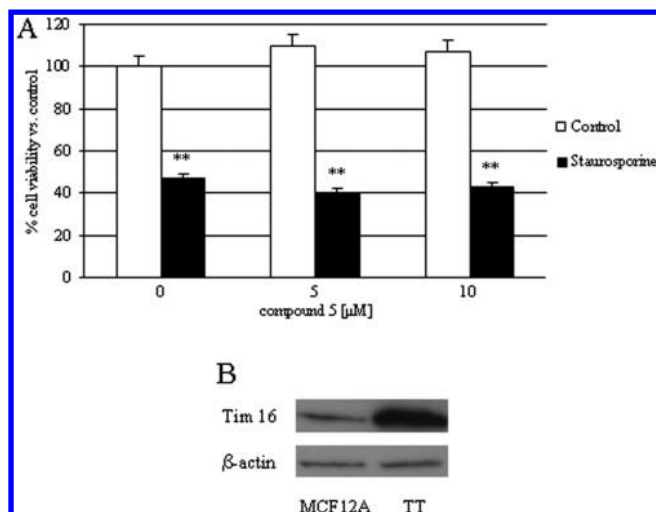


Figure 4. (A) Effects of compound 5 at 5 and 10 μ M in combination with staurosporine 50 nM on MCF12A cell viability. (B) Total proteins were isolated from MCF12A and from TT cells, and Western blot analysis for Tim 16 protein expression was performed. β -Actin is shown as loading control.

fluorescence consistent with a reduction in MMP. Compound 1 alone slightly affected MMP, as shown by the persistence of red fluorescence, consistent with a conserved MMP. On the contrary, TT cells treated with compound 5 showed a prevalent green fluorescence, indicating a drastic decrease in MMP. The latter was observed also after combined treatment with staurosporine and compound 1 or compound 5. These data

show that, as expected, staurosporine reduces MMP, a phenomenon observed also under treatment with compound 5 but not with compound 1, indicating that indeed compound 5 is acting at mitochondrial level. Compound 6 was also tested in MMP assay with no significant results (see Supporting Information page S17)

DISCUSSION AND CONCLUSION

The evidence that Magmas down-regulation sensitizes pituitary cells to proapoptotic stimuli prompted the search for chemical compounds that may be effective in reducing Magmas function. The availability of such compounds may indeed represent a powerful therapeutic tool to enhance tumor sensitivity to drugs inducing apoptosis, thereby contrasting the proliferative tumor potential. Our study provides the first evidence that a compound likely inhibiting Magmas protein, compound 5, is capable of sensitizing chemoresistant cells to proapoptotic stimuli without affecting cell viability per se. The latter evidence is of crucial importance for our study, since our aim was to identify a molecule devoid of toxic effects that could overcome resistance to proapoptotic stimuli. However, we cannot exclude that compound 5 may reduce cell viability and/or increase apoptosis in the cell line model at later time points. However, the lack of planarity of compound 5 does not make this compound a good candidate for DNA intercalation, which is, on the contrary, very likely for compound 1. Indeed, we show that compound 1 has direct cytotoxic effects, in keeping with previous evidence showing that compound 1 inhibits cell proliferation in yeast.¹¹

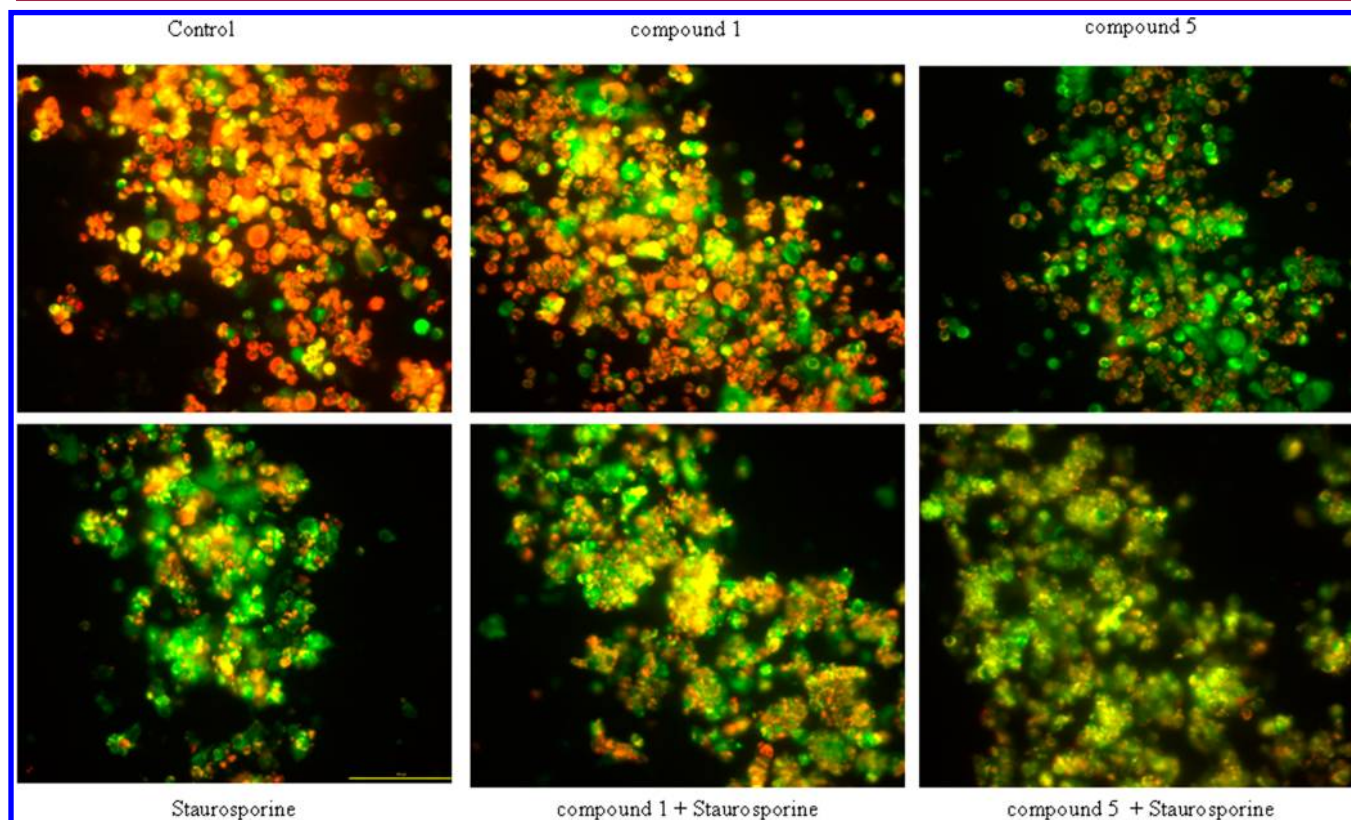


Figure 5. Mitochondrial membrane potential (MMP) evaluation. TT cells were treated with 50 nM staurosporine and with 5 or 10 μ M compound 1 or compound 5 alone or in combination. The red fluorescence corresponds to Jc-1 aggregates, indicating MMP activation. Green fluorescence indicates the presence of Jc-1 monomer, corresponding to a fall in MMP.

We here expand the SAR study of putative Magmas inhibitors by evaluating the importance of the guanidine residue for these compounds as chemosensitizers. Our study demonstrates that the guanidine moiety is crucial for the latter activity, since compounds **2**, **3**, and **4**, which are lacking this functionality, do not affect basal cell viability and apoptosis in TT cells and do not enhance the proapoptotic effects of a renowned apoptotic stimulus, such as staurosporine. Therefore, these data indicate that the guanidine moiety is fundamental for the chemosensitizing effects of Magmas inhibitors. We then evaluated the importance of planarity in the aliphatic portion of the molecule by studying the effects of compound **5**. Our results show that compound **5**, where planarity is lost, is indeed devoid of any cytotoxicity but is capable of enhancing the proapoptotic effects of staurosporine, indicating a better safety profile while the same chemical modification in the urea compound **6** did not elicit any activity. These data are in line with previous studies demonstrating that Magmas inhibition confers sensitivity to proapoptotic stimuli,^{3,4} suggesting that these compounds may be useful in association with classical chemotherapeutic drugs for cancer treatment. This strategy would allow a reduction of the chemotherapeutic agent effective dose, with a consequent decrease in side effect development.

The evidence that Tim 16 is overexpressed in neoplastic tissues^{2,3} suggests that this protein may represent a cancer biomarker, even if further studies are needed to support this hypothesis. However, the evidence that Tim 16 overexpression confers resistance to proapoptotic stimuli⁴ supports a role for this protein in cancer survival and progression.

Magmas protein lays in the mitochondrial inner membrane, where it takes part in the TIM23 complex, which in turn is fundamental for mitochondrial function preservation.¹³ It has been previously demonstrated that mitochondrial perturbation is critical for apoptosis in TT cells⁷ that express Tim 16, the protein encoded by Magmas. In addition, we have previously shown that Magmas overexpression enhances MMP and prevents the inhibitory effects of staurosporine on this parameter, indicating that Magmas is indeed involved in MMP control.⁴ Therefore, the evidence that treatment with compound **5** reduces MMP in TT cells provides further support for a mitochondrial involvement in the sensitizing effects of Magmas inhibitors. In addition, our results indicate that planarity is not important for the mitochondrial activity of the synthesized compounds, since compound **1** does not have a significant impact on MMP, in which perturbation, on the contrary, may be important for the sensitizing effects of Magmas inhibitors toward apoptotic stimuli. Our results indicate that compound **5** interacts with Magmas at the mitochondrial level, even if they do not rule out other possibilities. However, the hypothesis that compound **5** acts by influencing Tim 16 is supported by the evidence that compound **5** does not enhance the antiproliferative effects of staurosporine in the MCF12A cells, where Tim 16 is expressed at a very low level. Previous evidence showed that Magmas may also have a cytoplasmic localization,⁴ even if a cytoplasmic function for this protein is not known yet. Therefore, further studies are necessary to demonstrate the mitochondrial localization of compound **5** and its possible disruption of the TIM23 complex.

EXPERIMENTAL SECTION

All the reagents and solvents were of the highest quality available or were freshly distilled (Sigma-Aldrich, Milan, Italy). Melting points (uncorrected) were measured with a Buchi-Tottoli apparatus. ¹H, ¹³C, and bidimensional NMR spectra were recorded on a Varian 400 MHz instrument unless otherwise noted. Chemical shifts are given in ppm (δ) relative to the solvent, and coupling constants are in hertz. The abbreviation used are the following: s = singlet, d = doublet, t = triplet, q = quartet, dd = double doublet, m = multiplet, td = triple doublet, dt = double triplet, ddd = double double doublet. MS analyses were performed on a ESI Micromass ZMD 2000. HRMS results were recorded using a ESI-Q-TOF mass spectrometer (Agilent Technologies). Infrared spectra were recorded on a PerkinElmer FT-IR Spectrum 100 spectrometer. Flash chromatography was carried out on a silica gel (Merck, 230–400 mesh). HPLC analyses were performed using Beckman system Gold 168 using a C18 Jupiter column (150 mm \times 4.6 mm, 5 μ m) and water/acetonitrile/TFA eluent. Preparative HPLC results were recorded in a Waters Delta Prep 4000, using a C18 Jupiter column (250 mm \times 30 mm, 15 μ m) and water/acetonitrile/TFA eluent. The purity of all compounds was determined by HPLC (Beckman system Gold 168) and was greater than 95%.

Synthesis. *N*-[4-(3-Ethyl-2,4,4-trimethylcyclohex-2-enylidenemethyl)benzoyl]guanidine (**1**). The synthesis was as reported in ref 11a (**1**): C₂₀H₂₇N₃O mp = 125–130 °C. HRMS [MH]⁺ = 326.22 193. HRMS [MH]⁺ calcd = 326.222 69. ¹H NMR (400 MHz, acetone-*d*₆) δ 8.04 (br, 3H, NH), 7.98 (d, 2H, *J* = 8 Hz, CH₂Ar), 7.25 (d, 2H, *J* = 8 Hz, CH₂Ar), 6.50 (s, 1H, CH=Cq), 3.40 (br, NH), 2.63–2.60 (m, 2H, CH₂-CH₂-Cq=), 2.25 (q, 2H, *J* = 7.6 Hz, CH₂-CH₃), 1.91 (s, 3H, CH₃-C=), 1.49–1.47 (m, 2H, CH₂-CH₂-C=), 1.08 (s, 6H, 2CH₃), 1.04 (t, 3H, *J* = 7.6 Hz, CH₂-CH₃). ¹³C NMR (100 MHz, acetone-*d*₆) δ 173.13 (NH-CO-Ar), 160.62 (NH₂-C=NH), 147.94 (CH₃CH₂-C=), 141.41 (2CqAr), 141.14 (CH₂-Cq=CH), 130.05 (2CH_{Ar}), 129.32 (2CH_{Ar}), 128.10 (CH₃-C=), 122.30 (CqAr-CH=Cq), 39.68 (CH₂-CH₂-C=), 36.46 (CH₃-Cq-CH₃), 28.02 (2CH₃-Cq), 24.98 (CH₂-CH₂-C=), 23.39 (CH₂-CH₃), 15.48 (CH₃-C=), 15.17 (CH₂-CH₃).

4-(3-Ethyl-2,4,4-trimethylcyclohex-2-enylidenemethyl)benzoic Acid (**2**). The synthesis was as reported in refs 11b and 11c (**2**): C₁₉H₂₄O₂, mp = 150–155 °C. ESI [MH]⁺ = 285.21. ¹H NMR (400 MHz, MeOD) δ 7.84 (d, 2H, *J* = 7.6 Hz, CH₂Ar), 7.20 (d, 2H, *J* = 7.6 Hz, CH₂Ar), 6.41 (s, 1H, CH=Cq), 2.54–2.52 (m, 2H, CH₂-CH₂-Cq=), 2.18 (q, 2H, *J* = 7.6 Hz, CH₂-CH₃), 1.85 (s, 3H, CH₃-C=), 1.45–1.42 (m, 2H, CH₂-CH₂-Cq=), 1.03 (s, 6H, CH₃-C-CH₃), 1.02 (t, 3H, *J* = 7.6 Hz, CH₂-CH₃). ¹³C NMR (100 MHz, MeOD) δ 148.59 (CH₃CH₂-C=), 142.91 (CO-CqAr), 142.13 (CH₂-Cq=CH), 134.92 (CqAr-CH=Cq), 130.12 (2CH_{Ar}), 129.75 (2CH_{Ar}), 128.41 (=Cq-CH₃), 122.17 (CqAr-CH=Cq), 40.10 (CH₂-CH₂-C=), 36.80 (CH₃-Cq-CH₃), 28.14 (2CH₃), 25.31 (CH₂-CH₂-C=), 23.73 (CH₂-CH₃), 15.48 (CH₃-C= or CH₃-CH₂), 15.21 (CH₃-CH₂ or CH₃-C=). IR: cm⁻¹ 2958.76 C–H stretching, 1669.14 C=O stretching, 1589.06 C=C stretching, 961–610 C–H bending aromatic ring. X-ray crystal data: C₁₉H₂₄O₂; triclinic; space group *P* $\bar{1}$; *Z* = 2; *a* = 7.1637(2) Å, *b* = 7.6937(2) Å, *c* = 14.8938(4) Å, α = 82.749(1)°, β = 81.158(1)°, γ = 88.023(1)°; *V* = 804.54(4) Å³; Mo K α radiation θ_{\max} = 27.5°; 3635 unique reflections measured; 2892 observed reflections [*I* > 2 σ (*I*)]; final *R* index = 0.0518 (observed reflections), *R*_w = 0.1518 (all reflections).

4-(3-Ethyl-2,4,4-trimethylcyclohex-2-enylidenemethyl)benzamide (**3**). To a stirred solution of (**2**) (60 mg, 0.21 mmol) in DMF (5 mL), carbonyldiimidazole (CDI) (37.4 mg, 0.23 mmol) and concentrated NH₄OH (1.2 equiv) were added. After 24 h at room temperature, the reaction was monitored by mass spectrometry. The solvent was evaporated in vacuo, and the residue was crystallized from ether and centrifuged to yield the product as a yellow solid (**3**) (yield 20%). **3**: C₁₉H₂₅NO; mp over 220 °C. ESI [MH]⁺ = 284.25. HRMS [MH]⁺ = 284.293 53. HRMS [MH]⁺ calcd = 284.2009. ¹H NMR (400 MHz, DMSO) δ 7.81 (m, 4H, 2CH₂Ar and NH₂), 7.18 (d, 2H, *J* = 8.2 Hz, 2CH₂Ar), 6.41 (s, 1H, CH=Ph), 2.54–2.51 (m, 2H, CH₂-CH₂-Cq=), 2.15 (q, 2H, *J* = 7.5 Hz, CH₂-CH₃), 1.83 (s, 3H, CH₃-C=), 1.43–1.40

(m, 2H, $\text{CH}_2\text{-CH}_2\text{-Cq=}$), 1.03 (s, 6H, $\text{CH}_3\text{-C-CH}_3$), 1.00 (t, 3H, $J = 7.6$ Hz, $\text{CH}_2\text{-CH}_3$). ^{13}C NMR (100 MHz, DMSO) δ 169.85 ($\text{NH}_2\text{-CO-Ar}$), 146.81 ($\text{CH}_3\text{CH}_2\text{C=}$), 139.27 (CO-C_{qAr}), 138.76 ($\text{C}_{\text{qAr-CH}}$), 137.38 (CH=C_{qAr}), 129.28 (CH_{Ar}), 128.76 (CH_{Ar}), 128.00 (CH_{Ar}), 126.69 ($\text{=C}_{\text{qAr-CH}_3}$), 125.04 (CH_{Ar}), 121.40 ($\text{C}_{\text{qAr-CH=Cq}}$), 38.33 ($\text{CH}_2\text{-CH}_2\text{-C=}$), 35.43 ($\text{CH}_3\text{-C}_{\text{qAr-CH}_3}$), 27.47 (2CH_3), 23.78 ($\text{CH}_2\text{-CH}_2\text{-C=}$), 22.31 ($\text{CH}_2\text{-CH}_3$), 14.92 ($\text{CH}_3\text{-C=}$ or $\text{CH}_3\text{-CH}_2$), 14.73 ($\text{CH}_3\text{-CH}_2$ or $\text{CH}_3\text{-C=}$). IR: 2966.39 C–H stretching benzene, 1583.04, 1543.12 N–H bending.

[4-(3-Ethyl-2,4,4-trimethylcyclohex-2-enylidenemethyl)benzoyl]urea (4). To a solution of **2** (80 mg, 0.282 mmol) in azeotropic toluene (5 mL), urea (3.61 mg, 0.282 mmol) and the catalyst 3,4,5-trifluoromethylphenylboronic acid (3.61 mg, 0.310 mmol) were added. The mixture was stirred at reflux for 24 h. After this time, the reaction was monitored by TLC (AcOEt/EtPt 0.2:9.8) and mass spectrometry. At the end of the reaction toluene was removed in vacuo. The residue was solubilized with AcOEt and washed with NaHCO_3 (5%). The organic phase was dried and evaporated to dryness. The crude product was purified by preparative HPLC. **4**: $\text{C}_{20}\text{H}_{26}\text{N}_2\text{O}_2$, ESI $[\text{MH}]^+ = 327.14$. HRMS $[\text{MH}]^+ = 327.205$ 20. HRMS $[\text{MH}]^+$ calcd = 327.2073. ^1H NMR (400 MHz, CDCl_3) δ 8.05 (d, 2H, $J = 8.4$ Hz, CH_{Ar}), 7.36 (d, 2H, $J = 8.2$ Hz, CH_{Ar}), 6.47 (s, 1H, $\text{Ph-CH=C}_{\text{qAr}}$), 2.75–2.51 (m, 2H, $\text{CH}_2\text{-CH}_2\text{-C=}$), 2.23 (q, 2H, $J = 7.5$ Hz, $\text{CH}_2\text{-CH}_3$), 1.92 (s, 3H, $\text{CH}_3\text{-C=}$), 1.56–1.44 (m, 2H, $\text{CH}_2\text{-CH}_2\text{-C=}$), 1.15–1.02 (m, 9H, 3CH_3). ^{13}C NMR (100 MHz, CDCl_3) δ 171.44 (NH-CO-Ph), 149.51 ($\text{NH}_2\text{-CO-NH}$), 149.24 ($\text{CH}_3\text{CH}_2\text{C=}$), 144.95 (CO-C_{qAr}), 142.72 ($\text{CH}_2\text{-C}_{\text{qAr-CH}}$), 130.02 (2CH_{Ar}), 129.38 (2CH_{Ar}), 127.14 ($\text{CH}_3\text{-C=}$), 126.32 ($\text{C}_{\text{qAr-CH=}}$), 120.62 ($\text{C}_{\text{qAr-CH=Cq}}$), 38.92 ($\text{CH}_2\text{-CH}_2\text{-C=}$), 36.05 ($\text{CH}_3\text{-C}_{\text{qAr-CH}_3}$), 27.78 ($2\text{CH}_3\text{-Cq}$), 24.49 ($\text{CH}_2\text{-CH}_2\text{-C=}$), 23.10 ($\text{CH}_2\text{-CH}_3$), 15.37 ($\text{CH}_3\text{-C=}$), 14.87 ($\text{CH}_2\text{-CH}_3$).

N-[4-(3-Ethyl-2,4,4-trimethylcyclohexylmethyl)benzoyl]guanidine (5). To a solution of **1** (1.5 g, 4.8 mmol) in EtOH/AcOEt (1:1) (20 mL) was added 10% Pd/C, and the mixture was stirred under a hydrogen atmosphere (1 atm) until the theoretical amount of hydrogen gas was consumed. The reaction was monitored by mass spectrometry. At the end of the process the mixture was filtered, and the filtrate was concentrated. The residue was recrystallized from diethyl ether to afford 1.5 g (97% yield) of **5**: $\text{C}_{20}\text{H}_{31}\text{N}_3\text{O}$; mp = 118–121 °C. ESI $[\text{MH}]^+ = 330.25$. HRMS $[\text{MH}]^+ = 330.253$ 08. HRMS $[\text{MH}]^+$ calcd = 330.2545. ^1H NMR (400 MHz, MeOD) δ 7.94–7.90 (m, 2H, CH_{Ar}), 7.30–7.23 (m, 2H, CH_{Ar}), 3.43 (s, 1H, NH guanidine), 3.01 (dd, 1H, $J = 13.2$ Hz, $J = 5.0$ Hz, $-\text{CH}_2\text{-Bn}$), 2.62 (ddd, 2H, $J = 21.8$ Hz, $J = 13.4$ Hz, $J = 7.6$ Hz, $-\text{CH}_2\text{-Ph}$), 1.26–0.8 (m, 20H, aliphatic). ^{13}C NMR (100 MHz, MeOD) δ 171.55 (NH-CO-Ph), 168.64 ($\text{NH}_2\text{-C=NH}$), 146.85 (C_{qAr}), 131.42 (C_{qAr}), 129.39 (CH_{Ar}), 129.28 (CH_{Ar}), 128.84 (CH_{Ar}), 127.95 (CH_{Ar}), 60.11, 52.72, 38.44, 31.45, 27.16, 27.00, 23.93, 19.43, 18.80, 13.91.

[4-(3-Ethyl-2,4,4-trimethylcyclohexylmethyl)benzoyl]urea (6). To a solution of **4** (0.1 g, 0.302 mmol) in EtOH/AcOEt (1:1) (5 mL) was added 10% Pd/C, and the mixture was stirred under a hydrogen atmosphere (1 atm) until the theoretical amount of hydrogen gas was consumed. The reaction was monitored by mass spectrometry. At the end of the process the mixture was filtered, and the filtrate was concentrated. The residue was recrystallized from diethyl ether to afford compound **6** in 82% yield: $\text{C}_{20}\text{H}_{30}\text{N}_2\text{O}_2$; mp = 160–165 °C. HRMS $[\text{MH}]^+ = 331.237$ 60. HRMS $[\text{MH}]^+$ calcd = 331.2386. ^1H NMR (400 MHz, DMSO) δ 7.84 (d, 2H, $J = 8.3$ Hz, CH_{Ar}), 7.30 (d, 2H, $J = 8.2$ Hz, CH_{Ar}), 3.50 (m, 2H, $\text{Ph-CH}_2\text{-Cy}$), 1.74 (m, 1H, CH aliphatic), 1.55–0.71 (m, 20H, aliphatic). ^{13}C NMR (100 MHz, DMSO) δ 167.21 (NH-CO-Ar), 146.63 ($\text{NH}_2\text{-CO-NH}$), 129.29 (C_{qAr}), 129.12 (CH_{Ar}), 129.06 (CH_{Ar}), 128.90 (CH_{Ar}), 128.16 (C_{qAr}), 128.12 (CH_{Ar}), 69.95, 51.95 ($\text{CH}_3\text{-Cq-CH}_3$), 51.00, 43.94, 42.05, 32.38, 27.73, 22.40, 18.62, 11.99, 8.30.

Cell Line Culture. TT cells were purchased from ATCC (American Type Culture Collection, Manassas, VA, USA; ATCC CRL-1803) and grown in F12 medium (Euroclone, Milano, Italy), supplemented with 10% fetal bovine serum, at 37 °C in a humidified atmosphere with 5% CO_2 , as previously described.^{14,15}

The nontumorigenic breast epithelial MCF-12A cell line was purchased from the ATCC and grown as previously described.¹⁶

Western Blot Analysis. Human normal thyroid tissue was obtained from patients undergoing surgery for thyroid cancer and collected as previously described.^{17,18} The tissues were disrupted by using TissueRaptor (Qiagen, Milano, Italy) according to the manufacturer's instruction. For immunoblotting, human normal thyroid tissue and cell lines were dissolved in RIPA buffer (Pierce, Rockford, IL) and treated as previously described.¹⁹ Briefly samples were kept in ice for 30 min and then centrifuged for 10 min. The supernatant, containing the proteins, was then transferred to a new tube, and protein concentration was measured by BCA protein assay reagent kit (Pierce, Rockford, IL, USA), as previously described.⁴ For protein evaluation, lysates were fractionated on 10% SDS–PAGE, as previously described,²⁰ and transferred by electrophoresis to nitrocellulose transfer membrane (PROTRAN, Dassel, Germany). Membranes were incubated with 1:1000 polyclonal rabbit anti-Tim 16 (PRIMM, Milano, Italy). Anti-rabbit horseradish peroxidase-conjugated IgG antibody (Dako Italia, Milano, Italy) was then used at 1:5000, and binding was revealed using enhanced chemiluminescence (Pierce). The blots were then stripped and used for further blotting with 1:1000 polyclonal rabbit anti-human β -actin (Cell Signaling, Beverly, MA, USA).

Viable Cell Number Assessment. Variations in viable cell number were assessed by the ATPlite kit (PerkinElmer Life Sciences, MA, USA), seeding 2×10^4 cells/well in 96-well white plates, as previously described,²¹ and treated with the indicated compounds for 72 h. Control cells were treated with vehicle alone (0.1% DMSO). After incubation, the revealing solution was added and the luminescent output (relative luminescence units, RLU) was recorded using the Envision multilabel reader (PerkinElmer, Monza, Italy). Results are expressed as mean value \pm SE percent RLU vs vehicle-treated control cells from three independent experiments in six replicates.

Caspase Activity Assay. Caspase activity was measured by using Caspase-Glo 3/7 assay (Promega, Milano, Italy), as previously described.²² Briefly, 2×10^4 cells/well were seeded in 96-well white-walled plates and treated with the indicated compounds for 72 h. Then caspase-Glo 3/7 reagent was added at room temperature directly to the cell culture plates, which were shaken at 12.5g for 30 s, incubated for 1 h, and then measured for luminescent output (RLU) by the Envision multilabel reader (PerkinElmer). Results are expressed as mean value \pm SE percent RLU vs vehicle-treated control cells from three independent experiments in six replicates.

Mitochondrial Membrane Potential Evaluation. TT cells were treated without or with 50 nM staurosporine and 5 or 10 μM compound **1** or compound **5**, alone or in combination. MMP was then evaluated by employing the JC-1 mitochondrial membrane potential assay kit, following manufacturer instruction (Cayman Europe, Tallin, Estonia). Briefly, MMP was determined by incubating the cells with JC-1 dye at 37 °C for 30 min. The fluorescence intensity was observed by fluorescent microscopy (Nikon Eclipse T1000, Tokio, Japan), as previously described.²³

Statistical Analysis. Concerning the results of cell viability and caspase 3/7 activation experiments, a preliminary analysis was carried out to determine whether the data sets conformed to a normal distribution, and a computation of homogeneity of variance was performed using Bartlett's test. The results were compared within each group and between groups using ANOVA. If the F values were significant ($P < 0.05$), Student's paired or unpaired t test was used to evaluate individual differences between mean values. P values of <0.05 were considered significant. For all the other experiments, Student's paired or unpaired t test was used to evaluate individual differences between mean values and P values of <0.05 were considered significant.

■ ASSOCIATED CONTENT

Supporting Information

NMR and HRMS characterization of compounds **1–6** and molecular formula strings in csv format. This material is available free of charge via the Internet at <http://pubs.acs.org>. Complete crystallographic data have been deposited with the

Cambridge Crystallographic Data Centre as supplementary publications number CCDC 970130. Copies of that data can be obtained, free of charge, via www.ccdc.cam.ac.uk/conts/retrieving.html or on application to CCDC, 12 Union Road, Cambridge CB2 1EZ, U.K. [fax: +44(0)-1223-336033, e-mail deposit@ccdc.cam.ac.uk].

AUTHOR INFORMATION

Corresponding Author

*Phone: +39 0532 455924. Fax: +39 0532 455953. E-mail: claudio.trapella@unife.it.

Author Contributions

[†]A.C.Z. and T.G. contributed equally to this work.

Notes

The authors declare no competing financial interest.

ACKNOWLEDGMENTS

This work was supported by grants from the Italian Ministry of University and Research (Grants FIRB RBAP11884M, RBAP1153LS, and RBFR109SBM for C.T.), Fondazione Cassa di Risparmio di Ferrara, and Associazione Italiana per la Ricerca sul Cancro (AIRC) in collaboration with Laboratorio in Rete del Tecnopolo "Tecnologie delle Terapie Avanzate" (LTTA) of the University of Ferrara.

ABBREVIATIONS USED

Magnas, mitochondria-associated protein involved in granulocyte-macrophage colony-stimulating factor signal transduction; ACTH, adrenocorticotrophic hormone; MTC, medullary thyroid carcinoma; GH, growth hormone; NT, normal thyroid tissue; MMP, mitochondrial membrane potential

REFERENCES

- (1) Mokranjac, D.; Berg, A.; Adam, A.; Neupert, W.; Hell, K. Association of the Tim14.Tim16 subcomplex with the TIM23 translocase is crucial for function of the mitochondrial protein import motor. *J. Biol. Chem.* **2007**, *282*, 18037–18045.
- (2) Jubinsky, P. T.; Short, M. K.; Mutema, G.; Morris, R. E.; Ciruolo, G. M.; Li, M. J. Magnas expression in neoplastic human prostate. *J. Mol. Histol.* **2005**, *36*, 69–75.
- (3) Tagliati, F.; Gentilin, E.; Buratto, M.; Molè, D.; degli Uberti, E. C.; Zatelli, M. C. Magnas, a gene newly identified as overexpressed in human and mouse ACTH-secreting pituitary adenomas, protects pituitary cells from apoptotic stimuli. *Endocrinology* **2010**, *151*, 4635–4642.
- (4) Tagliati, F.; Gagliano, T.; Gentilin, E.; Minoia, M.; Molè, D.; degli Uberti, E. C.; Zatelli, M. C. Magnas overexpression inhibits staurosporine induced apoptosis in rat pituitary adenoma cell lines. *PLoS One* **2013**, *8*, e75194.
- (5) Zatelli, M. C.; Luchin, A.; Piccin, D.; Tagliati, F.; Bottoni, A.; Vignali, C.; Bondanelli, M.; degli Uberti, E. C. Cyclooxygenase-2 inhibitors reverse chemoresistance phenotype in medullary thyroid carcinoma by a P-gp mediated mechanism. *J. Clin. Endocrinol. Metab.* **2005**, *90*, 5754–5760.
- (6) Mitsiades, N.; Poulaki, V.; Tseleni-Balafouta, S.; Koutras, D. A.; Stamenkovic, I. Thyroid carcinoma cells are resistant to FAS-mediated apoptosis but sensitive to tumor necrosis factor-related apoptosis-inducing ligand. *Cancer Res.* **2000**, *60*, 4122–4129.
- (7) Starenki, D.; Park, J. I. Mitochondria-targeted nitrooxide, Mito-CP, suppresses medullary thyroid carcinoma cell survival in vitro and in vivo. *J. Clin. Endocrinol. Metab.* **2013**, *98*, 1529–1540.
- (8) Carlomagno, F.; Salvatore, D.; Santoro, M.; de Franciscis, V.; Quadro, L.; Panariello, L.; Colantuoni, V.; Fusco, A. Point mutation of the RET proto-oncogene in the TT human medullary thyroid

carcinoma cell line. *Biochem. Biophys. Res. Commun.* **1995**, *207*, 1022–1028.

(9) Mazumdar, M.; Adhikary, A.; Chakraborty, S.; Mukherjee, S.; Manna, A.; Saha, S.; Mohanty, S.; Dutta, A.; Bhattacharjee, P.; Ray, P.; Chattopadhyay, S.; Banerjee, S.; Chakraborty, J.; Ray, A. K.; Sa, G.; Das, T. Targeting RET to induce medullary thyroid cancer cell apoptosis: an antagonistic interplay between PI3K/Akt and p38MAPK/caspase-8 pathways. *Apoptosis* **2013**, *18*, 589–604.

(10) Tuttle, R. M.; Ball, D. W.; Byrd, D.; Daniels, G. H.; Dilawari, R. A.; Doherty, G. M.; Duh, Q. Y.; Ehya, H.; Farrar, W. B.; Haddad, R. I.; Kandeel, F.; Kloos, R. T.; Kopp, P.; Lamonica, D. M.; Loree, T. R.; Lydiatt, W. M.; McCaffrey, J.; Olson, J. A., Jr.; Parks, L.; Ridge, J. A.; Shah, J. P.; Sherman, S. I.; Sturgeon, C.; Waguespack, S. G.; Wang, T. N.; Wirth, L. J. Medullary carcinoma. *J. Natl. Compr. Cancer Network* **2010**, *8*, 512–530.

(11) (a) Jubinsky, P. T.; Short, M. K.; Ghanem, M.; Das, B. C. Design, synthesis, and biological activity of novel Magnas inhibitors. *Bioorg. Med. Chem. Lett.* **2011**, *21*, 3479–3482. (b) Das, B. C.; Kabalka, G. W. Design and synthesis of (E)-4-((3-ethyl-2,4,4-trimethylcyclohex-2-enylidene)methyl)benzoic acid. *Tetrahedron Lett.* **2008**, *49*, 4695–4696. (c) Das, B. C.; Mahalingam, S. M.; Mohapatra, P. Design and synthesis of guanidine-containing novel retinoids. *Tetrahedron Lett.* **2009**, *50*, 5860–5863.

(12) Maki, T.; Ishihara, K.; Yamamoto, H. Arylboronic acid-catalyzed direct condensation of carboxylic acids with ureas. *Synlett* **2004**, *8*, 1355–1358.

(13) Meier, S.; Neupert, W.; Herrmann, J. M. Conserved N-terminal negative charges in the Tim17 subunit of the TIM23 translocase play a critical role in the import of preproteins into mitochondria. *J. Biol. Chem.* **2005**, *280*, 7777–7785.

(14) Zatelli, M. C.; Tagliati, F.; Taylor, J. E.; Piccin, D.; Culler, M. D.; degli Uberti, E. C. Somatostatin, but not somatostatin receptor subtypes 2 and 5 selective agonists, inhibits calcitonin secretion and gene expression in the human medullary thyroid carcinoma cell line, TT. *Horm. Metab. Res.* **2002**, *34*, 229–233.

(15) Zatelli, M. C.; Piccin, D.; Tagliati, F.; Bottoni, A.; Luchin, A.; degli Uberti, E. C. SRC homology-2-containing protein tyrosine phosphatase-1 restrains cell proliferation in human medullary thyroid carcinoma. *Endocrinology* **2005**, *146*, 2692–2698.

(16) Minoia, M.; Gentilin, E.; Molè, D.; Rossi, M.; Filieri, C.; Tagliati, F.; Baroni, A.; Ambrosio, M. R.; degli Uberti, E.; Zatelli, M. C. Growth hormone receptor blockade inhibits growth hormone-induced chemoresistance by restoring cytotoxic-induced apoptosis in breast cancer cells independently of estrogen receptor expression. *J. Clin. Endocrinol. Metab.* **2012**, *97*, E907–E916.

(17) Rossi, R.; Zatelli, M. C.; Valentini, A.; Cavazzini, P.; Fallo, F.; del Senno, L.; degli Uberti, E. C. Evidence for androgen receptor gene expression and growth inhibitory effect of dihydrotestosterone on human adrenocortical cells. *J. Endocrinol.* **1998**, *159*, 373–380.

(18) Zatelli, M. C.; Piccin, D.; Tagliati, F.; Bottoni, A.; Luchin, A.; Vignali, C.; Margutti, A.; Bondanelli, M.; Pansini, G. C.; Pelizzo, M. R.; Culler, M. D.; degli Uberti, E. C. Selective activation of somatostatin receptor subtypes differentially modulates secretion and viability in human medullary thyroid carcinoma primary cultures: potential clinical perspectives. *J. Clin. Endocrinol. Metab.* **2006**, *91*, 2218–2224.

(19) Zatelli, M. C.; Luchin, A.; Tagliati, F.; Leoni, S.; Piccin, D.; Bondanelli, M.; Rossi, R.; degli Uberti, E. C. Cyclooxygenase-2 inhibitors prevent the development of chemoresistance phenotype in a breast cancer cell line by inhibiting glycoprotein p-170 expression. *Endocr.-Relat. Cancer* **2007**, *14*, 1029–1038.

(20) Zatelli, M. C.; Minoia, M.; Martini, C.; Tagliati, F.; Ambrosio, M. R.; Schiavon, M.; Buratto, M.; Calabrese, F.; Gentilin, E.; Cavalleco, G.; Berdondini, L.; Rea, F.; degli Uberti, E. C. Everolimus as a new potential antiproliferative agent in aggressive human bronchial carcinoids. *Endocr.-Relat. Cancer* **2010**, *17*, 719–729.

(21) Gagliano, T.; Bellio, M.; Gentilin, E.; Molè, D.; Tagliati, F.; Schiavon, M.; Cavalleco, N. G.; Andriolo, L. G.; Ambrosio, M. R.; Rea, F.; degli Uberti, E.; Zatelli, M. C. mTOR, p70S6K, AKT, and ERK1/2 levels predict sensitivity to mTOR and PI3K/mTOR

inhibitors in human bronchial carcinoids. *Endocr.-Relat. Cancer* **2013**, *20*, 463–475.

(22) Zatelli, M. C.; Gentilin, E.; Daffara, F.; Tagliati, F.; Reimondo, G.; Carandina, G.; Ambrosio, M. R.; Terzolo, M.; degli Uberti, E. C. Therapeutic concentrations of mitotane (o,p'-DDD) inhibit thyrotroph cell viability and TSH expression and secretion in a mouse cell line model. *Endocrinology* **2010**, *151*, 2453–2461.

(23) Molè, D.; Gentilin, E.; Gagliano, T.; Tagliati, F.; Bondanelli, M.; Pelizzo, M. R.; Rossi, M.; Filieri, C.; Pansini, G.; degli Uberti, E. C.; Zatelli, M. C. Protein kinase C: a putative new target for the control of human medullary thyroid carcinoma cell proliferation in vitro. *Endocrinology* **2012**, *153*, 2088–2098.